▌**Dendrimers**

Isolation and Characterization of Precise Dye/Dendrimer Ratios

Casey A. Dougherty,[a] Joseph C. Furgal,[a] Mallory A. van Dongen,[a] Theodore Goodson, III,[a] Mark M. Banaszak Holl,*[a] Janet Manono,[b] and Stassi DiMaggio*[b]

Abstract: Fluorescent dyes are commonly conjugated to nanomaterials for imaging applications using stochastic synthesis conditions that result in a Poisson distribution of dye/particle ratios and therefore a broad range of photophysical and biodistribution properties. We report the isolation and characterization of generation 5 poly(amidoamine) (G5 PAMAM) dendrimer samples containing 1, 2, 3, and 4 fluorescein (FC) or 6-carboxytetramethylrhodamine succinimidyl ester (TAMRA) dyes per polymer particle. For the fluorescein case, this was achieved by stochastically functionalizing dendrimer with a cyclooctyne "click" ligand, separation into sample containing precisely defined "click" ligand/particle ratios using reverse-phase high performance liquid chromatography (RP-HPLC), followed by reaction with excess azide-functionalized fluorescein dye. For the TAMRA samples, stochastically functionalized dendrimer was directly separated into precise dye/particle ratios using RP-HPLC. These materials were characterized using ^{1}H and ^{19}F NMR spectroscopy, RP-HPLC, UV/Vis and fluorescence spectroscopy, lifetime measurements, and MALDI.

Introduction

Precise control of dye/particle ratio has been a major challenge in nanomaterials chemistry.[1–4] For many classes of nanomaterials, there are a large number of functional sites to which a small number of ligands are conjugated. This results in a Poisson distribution of ligand/particle ratios in the product obtained. For example, a generation 5 poly(amidoamine) (G5 PAMAM) dendrimer with 128 surface sites will generate eight species ranging from 0 to 7 dyes per particle when an average of three dyes is conjugated to polymer (Figure 1). Although deviations from the Poisson distribution can arise from mass transport,[5] as well as site blocking and steric effects,[6] these detailed considerations tend to lead to broader, not narrower, distributions. The presence of these distributions complicates understanding the behavior of these materials and limits their effectiveness for desired applications.

Nanomaterials containing a Poisson distribution of dye/particle ratios have a range of photophysical and biodistribution properties. For this reason, a variety of strategies have been employed to minimize the distribution. A particularly interesting approach for dendrimeric polymers is encapsulation in the
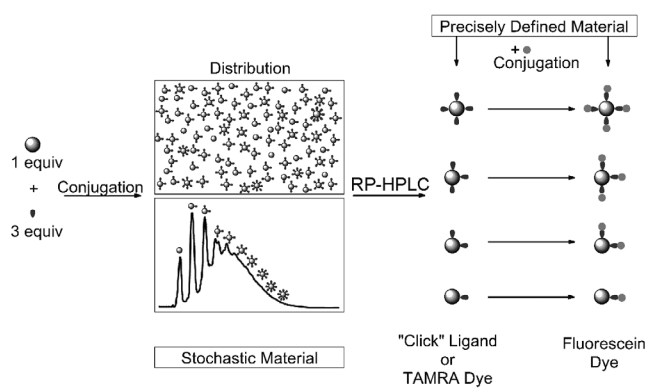
Figure 1. Outline of procedure for obtaining precise ligand/particle ratios on a G5 PAMAM dendrimer.

internal spaces between the branched arms.[7,8] Dye encapsulation can be tuned depending on concentration, dye structure, and dendrimer structure including generation, length of alkane linker in the core, and end-capping of arms.[7,9–11] Dendrimer structural isomerization can be used to vary the dye hosting capacity.[12] Computer simulations indicate that the dendrimer systems are dynamic and that no static encapsulation volumes exist within the dendrimer arms.[13]

In order to overcome the limitations of encapsulated and stochastically conjugated systems, effort has been invested to synthesize precise dye/particle ratios.[14–17] Convergent synthesis methods for dendritic polymers offer a powerful solution, although this strategy is generally limited to dye/particle ratios that are multiples of the numbers of dendrimer arms. Convergent strategies are also limited in terms of both dendrimer generation and molecular weight. Alternatively, methods to

[a] C. A. Dougherty, J. C. Furgal, Dr. M. A. van Dongen, Prof. T. Goodson, III, Prof. M. M. Banaszak Holl
Department of Chemistry, University of Michigan
Ann Arbor, Michigan, 48109-1055 (USA)
E-mail: mbanasza@umich.edu

[b] Dr. J. Manono, Prof. S. DiMaggio
Department of Chemistry, Xavier University
New Orleans, LA 70125 (USA)
E-mail: scdimagg@xula.edu

⊞ Supporting information for this article is available on the WWW under http://dx.doi.org/10.1002/chem.201304854.

give a unique conjugation site on the polymer, for example, the terminal site of a dendron, have also been employed.[18]

There is a substantial need for advance fluorescent probes with small dimensions (< 10 nm) and well-defined photophysical and biological properties.[19] We desired to develop a general strategy that would allow integer variation of dye/particle ratios on water soluble, divergent dendrimer platforms. In particular, the goal was to develop materials for which the dye/particle ratio was identical for all particles in the sample (precisely defined), as opposed to an average dye particle ratio made up of a Poisson distribution of materials (stochastic average). Dendrimers synthesized using divergent synthetic methods are generally more defective than convergent materials; however, a greater range of generations, and therefore sizes and molecular weight is available. Acetylated G5 PAMAM dendrimer was selected as a material target because it is large enough to impart aqueous stability to at least ten hydrophobic ligands while it is small enough to escape through vascular pores and disperse through the tissue matrix to reach cells.[20] In addition, it is small enough to be filtered and excreted by the kidneys. G5 and G6 PAMAM dendrimers with these properties were recently prepared using stochastic conjugations of Cy3 and Cy5 dyes.[21] The amine-terminated G5 PAMAM dendrimer is of interest because this material, which becomes positively charged in aqueous solution, is a useful nonviral vector for gene delivery.[22–24] For all of these biological applications, materials with homogenous photophysical and biodistribution properties that also meet the biological criteria discussed above are desired. For this combined set of reasons, we desired to find a solution to obtaining precise ligand/dendrimer ratio materials for divergent, hydrophilic dendrimers.

Recently, we reported isolating materials with systematic variation of "click ligand"/dendrimer ratio on a G5 PAMAM core.[25] This system is interesting in that dendrimer samples containing precise ligand/particle ratio can be isolated even though the divergent G5 dendrimer platform itself retains its normal molecular weight distribution. This suggested two possible paths for obtaining G5 PAMAM dendrimer materials containing precise dye/particle ratios: 1) dye conjugation to materials containing precise click ligand/dendrimer ratios or 2) isolation by direct separation of a stochastic mixture of dye conjugates. We now report the successful isolation of G5-(FC)$_n$ ($n = 1$–4) using the click conjugation strategy and G5-TAMRA$_n$ ($n = 1$–3) using the direct separation of dye conjugates.

Results and Discussion

Conjugation of small numbers of hydrophobic ligands, including click linkers or dyes, to G5 PAMAM dendrimer generates a Poisson distribution of ligand/particle ratios (Scheme 1a and Scheme 2a).[1,2] As highlighted in Scheme 1b and Scheme 2b,
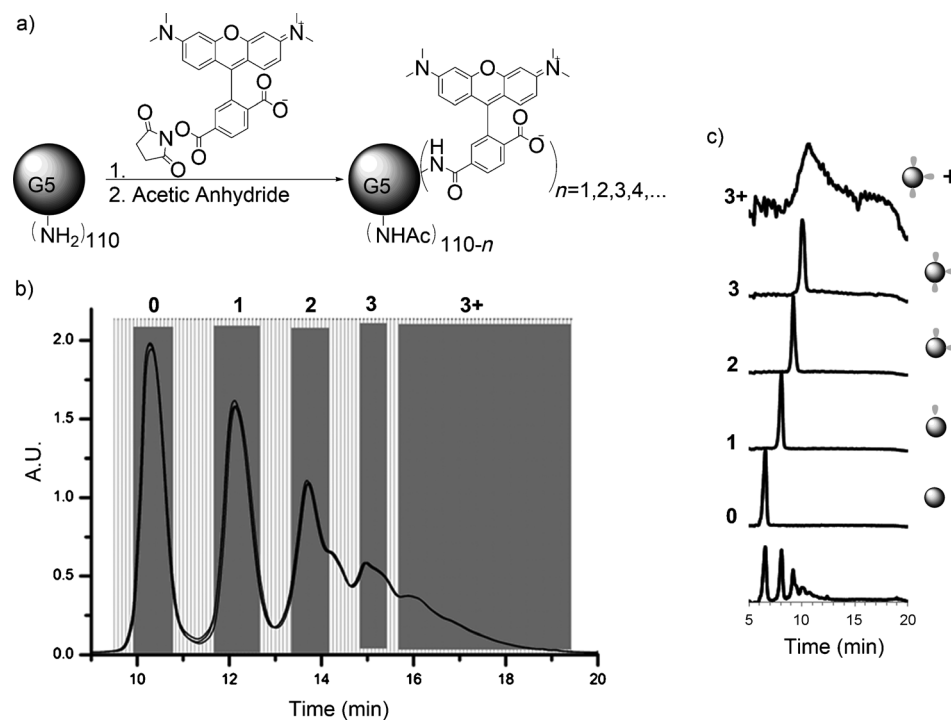
Scheme 1. Isolation of dendrimer conjugates G5-Ac-TAMRA$_n$ by semipreparative RP-HPLC. a) Conjugation and full acetylation of G5-Ac-TAMRA$_n$. b) Overlay of semipreparative RP-HPLC traces for two individual runs. Fractions selected for each dendrimer/ligand component are highlighted. c) RP-UPLC traces for the isolated dendrimer conjugates (each trace is baseline corrected and normalized). Both RP-HPLC and RP-UPLC traces detected at 210 nm.

the amount of shift induced on a C18 RP-HPLC column by each hydrophobic ligand is substantially greater than the peak width induced by the mass distribution of the dendrimer. The baseline separation achieved for the isolated fractions is substantially improved over previous reports[25] because a more highly purified monomer of G5 PAMAM dendrimer was employed from which dimer, trimer, and all trailing generations have been removed by semipreparative RP-HPLC (Schemes 1c and Scheme 2c).[26] The tail end of the G5-Ac-TAMRA stochastic mixture (3+ trace in Scheme 1c) was combined to generate a mixture of G5-TAMRA conjugates containing ≥ 3 TAMRA dye/dendrimer particles.

RP-UPLC indicates the successful isolation of G5-Ac-TAMRA$_1$, G5-Ac-TAMRA$_2$, and G5-Ac-TAMRA$_3$ as discrete samples containing precise dye/dendrimer ratios within the error of the method (Scheme 1c). No shoulders are present on the traces, which would indicate a mixture of ligand/particle ratios, as we have both seen and quantitatively analyzed in previous stud-
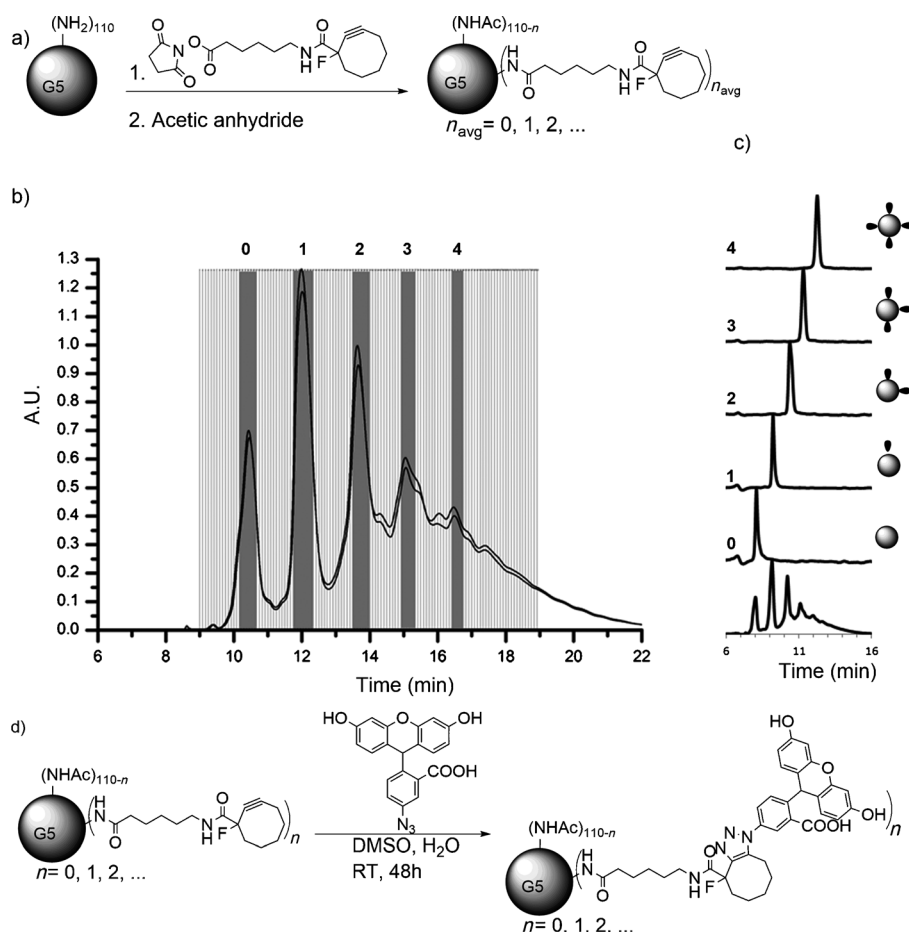
Scheme 2. Isolation of dendrimer conjugates G5-Ac-MFCO$_n$ by semipreparative RP-HPLC. a) Conjugation and full acetylation of G5-Ac-MFCO$_n$. b) Overlayed semipreparative RP-HPLC traces from four individual runs. Fractions selected for each dendrimer/ligand component are highlighted. c) RP-UPLC traces for the isolated dendrimer conjugates (each trace is baseline corrected and normalized). d) Synthesis of precise ratio dendrimer conjugates G5-Ac-FC$_n$ by "click" reactions. Both RP-HPLC and RP-UPLC traces detected at 210 nm.

tration data to determine number of dendrimer arms propagates into the determination of NMR ratios. This NMR error is also not constant for each sample because the relative size of the collected fraction versus real RP-HPLC peak width varies. For these reasons, we believe the RP-UPLC data provide a better measure of the TAMRA/dendrimer ratio. The full defect structure of the G5 PAMAM dendrimer is subsumed in the RP-UPLC peak width and the peak-to-peak separation is determined by the number of conjugated hydrophobic ligands. Unlike the NMR analysis, this effectively decouples the RP-UPLC assessment of ligand/particle ratio from the base polymer defect structure. Baseline separation of the click ligand/dendrimer ratios is obtained for the isolated samples (Schemes 1 c and 2 c, Figure 2 a).

In order to generate the G5-Ac-FC$_n$ ($n=1$–4) samples and drive the click reaction to completion, each G5-Ac-MFCO$_n$ ($n=1$–4) was allowed to react with a tenfold excess of azido-fluorescein (based on the number of MFCO ligands). RP-UPLC characterization indicated the occurrence of successful click reaction

ies.[1] Each of these samples was also analyzed by ^{1}H NMR spectroscopy using methods described previously (Table S1 in the Supporting Information).[2,25] In order to evaluate relative integral values and estimate the TAMRA/dendrimer ratio, the acetyl methyl peak of the dendrimer at 1.8 ppm was set to a value of 279 protons based on the average number of 93 arms present for monomer-only G5 PAMAM as determined by gel-permeation chromatography (GPC) and titration.[2,26] The nine aromatic TAMRA protons were used to determine the relative amount of dye. This resulted in an NMR-based estimate of the TAMRA/dendrimer ratios of 0.7, 1.6, 3.1, and 4.4 for the G5-Ac-TAMRA$_1$, G5-Ac-TAMRA$_2$, G5-Ac-TAMRA$_3$, and G5-Ac-TAMRA$_{3+}$ samples, respectively. Unfortunately, the NMR analysis suffers in accuracy from the large difference in the number of dendrimer versus dye protons and the need to use an average value for the number of acetylated protons on the dendrimer.[2,25] In addition, the isolated precise ratio samples derive from only a subset of the full stochastic distribution generated by the synthesis (i.e., the gray bars in Schemes 1 b and 2 b extend over only part of the peak-width with this fraction decreasing as n increases). This error in the use of the GPC and ti-

whether the trace was detected at 210 nm (dendrimer backbone absorption) or at 491 nm (FC absorption; Figure 2). For both G5-Ac-FC$_3$ and G5-Ac-FC$_4$ a small amount of $n-1$ product was detected. Each dye/dendrimer ratio was characterized by ^{1}H NMR spectroscopy (Table S3 in the Supporting Information). The analysis was directly analogous to that described for the TAMRA case (with the same limitations) and resulted in FC/dendrimer ratios of 1.2, 1.8, 3.3, and 3.0 for the G5-Ac-FC$_1$, G5-Ac-FC$_2$, G5-Ac-FC$_3$, and G5-Ac-FC$_4$ samples, respectively. The MFCO ligand also provides the opportunity to analyze the materials using ^{19}F NMR spectroscopy. Spectra for G5-Ac-MFCO$_n$ ($n=1$–4; $\delta=-145.1$ ppm) exhibiting integrated ratios of 1.2, 2.2, 3.2 and 4 are illustrated in Figure 3 a. After conjugation with azide-FC, the peaks broaden, shift to $\delta=-145.8$ ppm, and give integrated ratios of 0.8, 1.6, 2.9 and 4. Note that the ^{19}F NMR analysis does not require the use of average dendrimer arm values but directly measures the number of conjugated arms per dendrimer, independent of structural defects in the polymer scaffold.

The decrease in intensity of the ^{19}F signal (Figure 3 b) upon clicking the dye to the cyclooctyne is only observed for dendri-
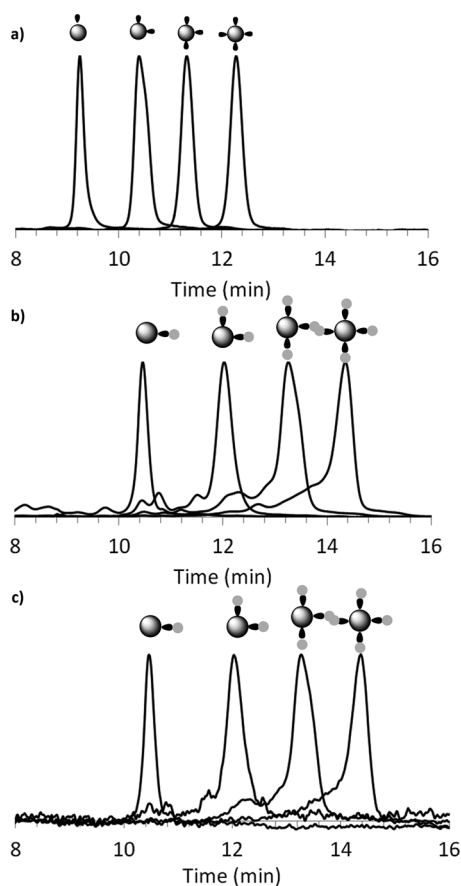
Figure 2. RP-UPLC traces of: a) G5-Ac-MFCO$_n$ ($n = 1$–4) at 210 nm, b) G5-Ac-FC$_n$ ($n = 1$–4) at 210 nm, c) G5-Ac-FC$_n$ ($n = 1$–4) at 491 nm.
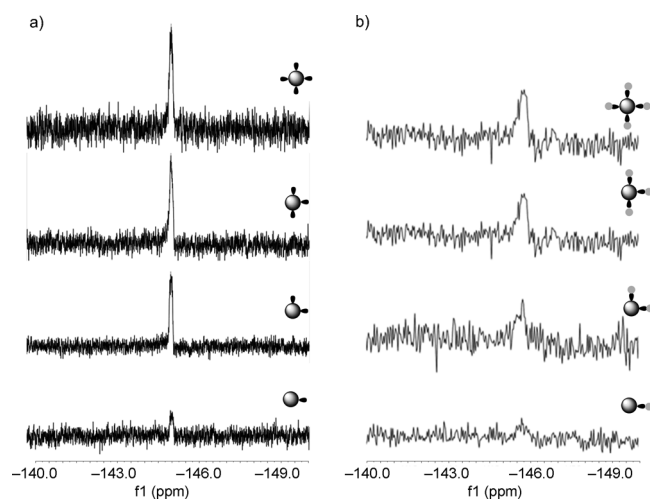

Figure 3. ^{19}F NMR spectroscopy of: a) pre-, and b) post-click reactions for G5-Ac-MFCO$_n$ and G5-Ac-Fc$_n$ ($n = 1$–4).

mer conjugates. For small molecule click reactions between the MFCO click ligand and fluorescein in the absence of dendrimer, the peak shifts and broadens but does not decrease in intensity (Figure S5 in the Supporting Information). Since the intensity decrease is unique to the dendrimer conjugates measured in both deuterated DMSO and water, it suggests this

change arises from the clicked ligand being internalized into the dendrimer. Hydrophobic dyes can be hosted in the branches of a dendrimer,[7,9,10,13] and it appears the addition of the fluorescein dye favors the fluorinated ligand to be internalized into the dendrimer. Disappearance of the fluorine signal of a small molecule upon encapsulation into a polyglycerol dendrimer has been previously reported.[30] We also observe a decrease in the fluorine signal for clicked small molecules as a stoichiometric amount of the G5 PAMAM dendrimer is added to the solution (Figure S6 in the Supporting Information) further supporting the encapsulation hypothesis. MALDI-TOF-MS measurements illustrate an overall increase in molecular weight of the polymer conjugates as a function of ligand number, n, for both fluorescein and rhodamine dendrimer samples (Tables S1 and S3 in the Supporting Information). The breadth of the molecular weight distribution for the G5 PAMAM polymer (Figure S1 in the Supporting Information)[31] limits the value of this approach for accurately determining the number of ligands present on each polymer particle. The defect structure of G5 PAMAM dendrimer results in a molecular weight distribution ranging from approximately 21 000 to 28 000 Da. The click ligand–FC and TAMRA conjugates have a mass of 707 and 527, respectively. As discussed for the NMR analysis, the isolated fractions do not account for the full stochastic distribution of products and will therefore introduce error into attempts using mass spectrometry data to assign ligand/dendrimer ratios. In addition, MALDI-TOF-MS shot noise for these samples is 660 Da, which is similar to the ligand mass. For these reasons, MALDI-TOF-MS is of limited use in assigning numbers of ligand per particle. MALDI-TOF-MS was of greater use in characterizing precise ratio clusters of G5 PAMAM dendrimers for which the mass shifts were approximately 30 000 Da.[31] The precise ratio G5(G5)$_n$ dendrimer clusters were generated using the same precise ratio linker samples illustrated in Scheme 2.
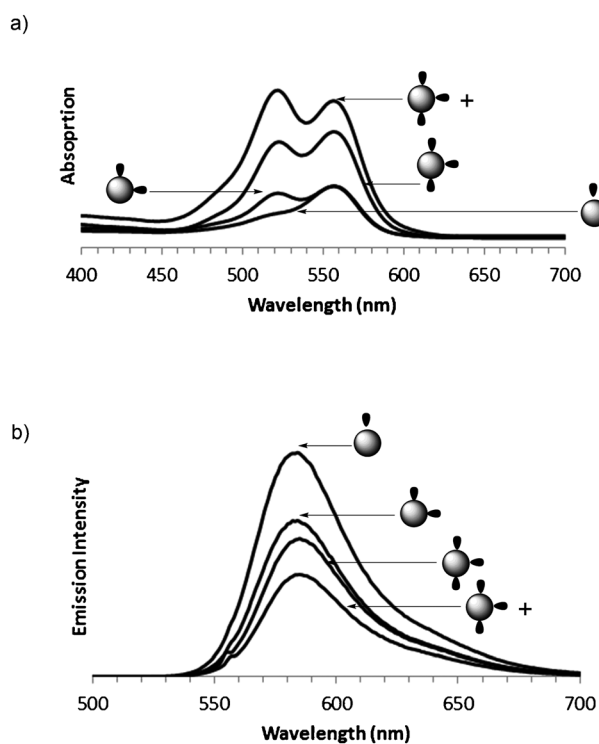
Both sets of precise dye/dendrimer ratio samples, G5-Ac-FC$_n$ ($n = 1$–4) and G5-Ac-TAMRA$_n$ ($n = 1$–3, 3 +), were characterized in terms of absorption and fluorescent emission. Absorption spectra of G5-Ac-FC$_n$ show the anticipated increase in intensity at 491 nm associated with the fluorescein dye, although the extinction coefficient does not vary linearly with concentration (Figure 4 and Table S4 in the Supporting Information). This nonlinearity is expected as these samples, although dilute in terms of polymer concentration, hold the conjugated dyes in close proximity to each other, and therefore, do not meet the criteria for Beer's law in terms of local dye concentration. These samples of 0.1 mg mL^{-1} concentration of polymer correspond to approximately 1×10^{-6} M polymer and dye for G5-Ac-FC$_n$ where $n = 1$; however for $n = 2$, 3, and 4 the local concentration of dye is roughly 9, 13.5 and 18 M, respectively. The emission spectra, centered at 526 nm, deviate even more strongly from a linear response as a function of n. The emission intensity of G5-Ac-FC$_3$ and G5-Ac-FC$_2$ are identical and the emission for G5-Ac-FC$_4$ is less intense than that observed for $n = 2$ or 3. These observations belie the general strategy that placing more dye on a dendrimer will result in greater emission intensity. Absorption spectra of the G5-Ac-TAMRA$_n$ sam-
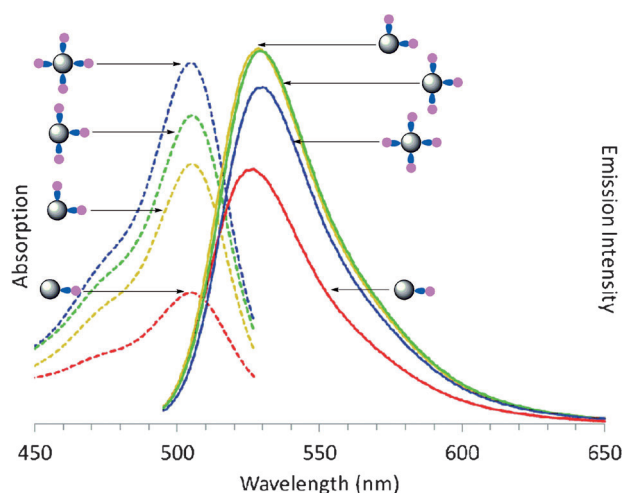
Figure 4. Absorption (dotted line) and emission (solid line) spectra of precisely defined G5-Ac-FC$_n$ ($n = 1$–4) conjugates (0.1 mg mL^{-1}).

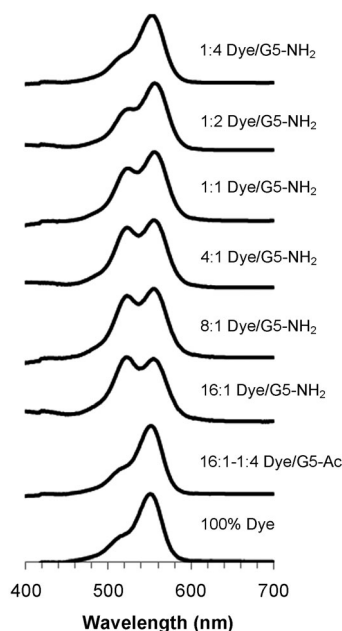ratio of TAMRA/dendrimer particles as opposed to a stochastic distribution. Note the G5-Ac-TAMRA$_2$ sample has a local dye concentration of about 9 M. This overall peak shape is also observed for G5-Ac-TAMRA$_3$ and the 520 nm peak supersedes the 555 nm peak in intensity for the G5-Ac-TAMRA$_{3+}$ sample. The fluorescence emission intensity shows an inverse relationship with the TAMRA/dendrimer ratio (Figure 5 b).

The absorption spectra of the G5-Ac-TAMRA$_n$ ($n = 1$–3, 3+) samples provide an opportunity to better understand the spectra obtained for fluorescent dye encapsulated in G5 dendrimer. By applying the data obtained from the absorption spectra of the precise ratio samples, we can better understand the physical encapsulation generated by physical mixing. A series of spectra are presented at a constant dye concentration of 3.0×10^{-6} M in water, which would normally result in a monomer absorption signature,[32] and the impact of dye encapsulation into the both G5-NH$_2$ and G5-Ac dendrimer is illustrated in Figure 6. At a 16:1 TAMRA/G5-NH$_2$ ratio, the 520 nm peak is

ples also deviate from a linear Beer's law response and exhibit a transition from monomer to dimer-like spectral bands that is consistent with the rhodamine small molecule absorption behavior reported as a function of concentration in solution (Figure 5 a).[32] The spectrum for G5-Ac-TAMRA$_1$ is identical to that observed for unconjugated TAMRA at a dye concentration of 3.0×10^{-6} M, known to give a monomer absorption spectra. The spectrum for G5-Ac-TAMRA$_2$ exhibits the increase in intensity at 520 nm associated the formation of TAMRA dimers and provides additional evidence that this sample contains a precise

a)

b)

Figure 5. a) Absorption, and b) emission and spectra of precisely defined G5-Ac-TAMRA$_n$ ($n = 1$–3, 3+) conjugates (0.1 mg mL^{-1}).

Figure 6. Absorption spectra of 3.0×10^{-6} M TAMRA dye in water with varying amounts of G5-NH$_2$ or G5-Ac added to solution. The TAMRA-only absorbance is at a concentration at which only monomer behavior is present. Once G5-NH$_2$ dendrimer is added the TAMRA becomes encapsulated and shows dimer-absorption behavior. The monomer-absorption behavior is not seen until a large excess of dendrimer has been added. The addition of G5-Ac does not cause any change in the absorption over the range of 16:1 to 1:4 dye/G5-Ac ratios.

more intense than the 550 nm peak, consistent with the conjugate containing 3+ TAMRA dye per dendrimer and an effective local dye concentration of >14 M. The 8:1 and 4:1 TAMRA/G5-NH$_2$ ratios have absorption peak shapes similar to the G5-Ac-TAMRA$_3$ conjugate. Interestingly, for all three ratios measured ranging from 16:1 to 4:1 TAMRA/G5-NH$_2$, the 550/520 nm peak ratio suggests little if any monomer TAMRA is present in solution. The 550/520 nm peak ratio for both the 1:1 and 1:2 TAMRA/G5-NH$_2$ ratios indicate that species contain-

ing both 1 and 2 encapsulated dye/dendrimer exist in solution. The intensity of the 550 nm peak definitively indicates that neither the stoichiometric 1:1 ratio, nor even the case in which there are two dendrimers for every dye, succeeds in generating a defined sample containing one dye encapsulated per dendrimer.

It is not until a fourfold excess of dendrimer is employed that the dye absorption spectrum is consistent with that of monomer dye. The absorption data indicate that mixtures of TAMRA/G5-NH$_2$ ratios are present even for the case of one dye per dendrimer. Therefore, similar to stochastic conjugation methods, physical encapsulation strategies also result in a mixture of small molecule/dendrimer ratios. Similar aggregation phenomena have been reported previously for the interaction of methylene blue with generations 1.5 to 7.5 PAMAM dendrimer terminated with carboxylic acid groups.[11] For this case involving a positively charged dye and negatively charged dendrimer, monomer, dimer, and higher aggregates were observed. For the interaction of neutral G5-Ac with TAMRA, the absorption data for all ratios of TAMRA/G5-Ac, 16:1 to 1:4, only the monomer absorption was observed (Figure 6). This suggests that although it is favorable for TAMRA to intercalate into the G5-NH$_2$ dendrimer for a water solution, intercalation into the G5-Ac dendrimer does not occur or is limited to a single dye. This difference is consistent with previous observations that amine-terminated PAMAM dendrimer in water is extended with available volume between the arms if solvent is displaced whereas acetylated PAMAM is a compact, condensed structure with little available volume.[33]

In order to better understand the trends in the absorption and emission spectra of the fluorescein samples, we also carried out fluorescence lifetime as well as quantum yield measurements. The fluorescence lifetime measurements were carried out with femtosecond fluorescence upconversion spectroscopy, which is very sensitive to small changes in the decay rates. The lifetime data suggest a two-component decay with an initial short relaxation time on the order of about 15 ps and a longer decay of approximately 200 ps (Table 1). In addition to

Table 1. Fluorescence lifetime kinetic data for G5-Ac-MFCO-FC$_n$ ($n = 1$–4) samples.

Fluoresceins per G5	QY [%]	Short [ps]	Long [ps]	R^2
1	21 ± 2	13 ± 2	199 ± 40	0.94
2	20 ± 1	14 ± 1	188 ± 19	0.98
3	13 ± 1	15 ± 1	166 ± 21	0.99
4	14 ± 1	11 ± 1	155 ± 9	0.99
fluorescein	79	8.5 ± 1.3	223 ± 36	0.93

this overall decay profile, the G5-Ac-FC$_1$ and G5-Ac-FC$_2$ samples have long decay components close to approximately 200 ps, whereas those for G5-Ac-FC$_3$ and G5-Ac-FC$_4$ appeared to have shorter decay components (~165 ps), albeit within the error the measurement. This possible difference between the G5-Ac-FC$_1$/G5-Ac-FC$_2$ and G5-Ac-FC$_3$/G5-Ac-FC$_4$ samples is also supported by a similar trend in the quantum yield. Combining

these two results suggests that the decrease in the quantum yield observed for the G5-Ac-FC$_3$ and G5-Ac-FC$_4$ is related to the increased decay rate of these samples. Physically, the average distance between chromophores is becoming smaller in these samples and the possibility of chromophore–chromophore interactions and promotion of nonradiative pathways in the system is increased. This type of trend has been observed previously for chromophores stochastically attached to dendrimers in which the increased loading of the chromophores on the surface of the dendrimer was not linear in terms of the quantum yield or fluorescence lifetime with number of chromophores.[34–36] Attempts to obtain lifetime data for these TAMRA samples were unsuccessful due to poor overlap of the laser emission with the TAMRA absorption. Quantum yield data showed the expected decrease as the number of TAMRA dyes per particle increased (Table S5 in the Supporting Information).

Conclusion

In summary, two approaches to the formation of G5 PAMAM samples containing precise dye/dendrimer ratios have been presented. The first approach, using direct separation based on dye hydrophobicity, generated a set of TAMRA containing dendrimer, G5-Ac-TAMRA$_n$ ($n = 1$–3, 3+). The second approach, using click chemistry strategy, generated a set of fluorescein containing dendrimer, G5-Ac-FC$_n$ ($n = 1$–4), using a method that could be readily extended to any azide-containing dye or other desired functional group. Both absorption and emission spectra show a strong dependence on the dye/dendrimer ratio.

Experimental Section

Biomedical grade G5 PAMAM dendrimer was purchased from Dendritech Inc., and purified using RP-HPLC to obtain G5 dendrimer without trailing generations (G1–G4), dimers, and trimers.[26] Aminofluorescein, trifluoroacetic acid, triethylamine, and acetic anhydride were purchased from Sigma–Aldrich (St. Louis, MO) and used as received. HPLC grade water, acetonitrile, and methanol, as well as dimethyl sulfoxide, hydrochloric acid, sodium azide, and sodium nitrite, were purchased from Fisher-Scientific and used as received. Click-Easy™ MFCO-N-hydroxysuccinimide was purchased from Berry & Associates Synthetic Medicinal Chemistry (Dexter, MI) and used as received. 5-Carboxytetramethylrhodamine (TAMRA) succinimidyl ester was purchased from Life Technologies and was used as received. Azido-fluorescein was synthesized using a literature protocol.[27] A 500 MHz Varian NMR instrument was used for all ^{1}H and ^{19}F NMR measurements. [19]F spectra were referenced to the ^{19}F signal of internal trichlorofluoromethane using a Ξ of 94.0940110. All MALDI-TOF-MS measurements were performed on a Bruker Ultraflex III.

Synthesis of G5-Ac-MFCO conjugates (stochastic average)

MFCO-N-hydroxysuccinimide (0.0062 g, 0.0240 mmol, 4.4 equiv) was dissolved in dimethyl sulfoxide (1.6 mL) and added dropwise to a solution of G5 PAMAM dendrimer (0.1554 g, 0.0055 mmol, 1.0 equiv) in water (34.4 mL). The mixture was stirred at 21 °C, overnight, and purified by centrifuge washing twice with 1×PBS and

five times with deionized water. Upon lyophilization a white solid was obtained (61% yield). The white solid (0.0936 g, 0.0033 mmol, 1.0 equiv) was dissolved in anhydrous methanol (17.3 mL), triethylamine (0.11 mL) was added (0.07 mol, 224 equiv), and the mixture was stirred for 15 min. Acetic anhydride (0.06 mL, 0.60 mmol, 179 equiv) was added slowly until the solution turned clear and the mixture was stirred at room temperature for 4 h. The sample was lyophilized, dissolved in 1×PBS (2.5 mL), and purified using centrifuge washing twice with 1×PBS and five times with deionized water. Upon lyophilization a white solid was obtained (73% yield).

Synthesis of G5-Ac-TAMRA conjugates (stochastic average)

TAMRA succinimidyl ester (0.0102 g, 0.0194 mmol, 3.5 equiv) was dissolved in dimethyl sulfoxide (2.5 mL), added dropwise to G5 PAMAM dendrimer (0.1520 g, 0.0054 mmol, 1.0 equiv) dissolved in water (33.7 mL), and stirred at 21 °C, overnight. The reaction mixture was passed through a Sephadex column (GE Healthcare protocol) to remove unreacted TAMRA and lyophilized, resulting in a purple solid (78% yield). The purple solid (0.1178 g, 0.0042 mmol, 1.0 equiv) was dissolved in anhydrous methanol (22.4 mL), 0.15 mL triethylamine (0.09 mol, 224 equiv) was added, and the mixture was stirred for 15 min. Acetic anhydride (0.08 mL, 0.8 mmol, 179 equiv) was added slowly until the solution became transparent. The mixture was stirred at 21 °C for 4 h and lyophilized. The sample was redissolved in 1×PBS (2.5 mL) and purified using centrifuge washing twice with 1×PBS and five times with deionized water. Upon lyophilization, a purple solid was obtained (72% yield).

Isolation of precise ratio G5-Ac-MFCO$_n$ ($n = 1$–4)

RP-HPLC separation was carried out using a Waters Delta 600 HPLC with a C18 silica-based RP-HPLC column (250×21.20 mm, 5 μm particles) connected to a C18 guard column (50×21.20 mm). The mobile phase consisted of a linear gradient beginning with 95:5 (v/v) water/acetonitrile mixture and ending with 55:45 (v/v) water/acetonitrile over 30 min at a flow rate of 16.37 mL min^{-1}. The water/acetonitrile mixture contained 0.10 wt% trifluoroacetic acid (TFA). Elution traces of the dendrimer–ligand conjugate were obtained at 210 nm. A concentration of 30 mg mL^{-1} per injection was used. The autosampler fractions were 5 s long and 120 fractions were collected starting at 9 min and 1 s. The fractions were then combined to obtain each G5-Ac-MFCO$_n$ sample based upon analysis of the chromatogram in Origin-Pro.

General procedure for copper-free click reactions

A stock solution of azido-fluorescein (54 mM) in dimethyl sulfoxide was prepared. Each G5-Ac-MFCO$_n$ was dissolved in methanol at a concentration of 2 mM based on MFCO. Ten equivalents of azido-fluorescein per each MFCO were added and the mixture was stirred at 21 °C for 48 h. Following lyophilization the solid was redissolved in 10×PBS (2.5 mL), eluted through a Sephadex column (GE Healthcare protocol) to remove excess azido-fluorescein. The total solution (3.5 mL) was transferred to a 10 000 molecular cutoff dialysis bag (10 mL) and dialyzed versus two rounds of nanopure water (1 L). Lyophilization resulted in an orange solid.

Isolation of precise ratio G5-Ac-TAMRA$_n$ ($n = 1$–3, 4+)

General RP-HPLC protocols and solvents were identical to those described above. A concentration of 25 mg mL^{-1} per injection was

used. The autosampler fractions were 5 s long and 120 fractions are collected starting at 10 min and 1 s. The fractions were then combined to obtain each G5-Ac-TAMRA$_n$ sample based upon analysis of the chromatogram in Origin-Pro.

Analytical reverse-phase ultrahigh performance liquid chromatography (RP-UPLC)

A Water Acuity system with a C18 silica-based UPLC column (Agilent) was employed with a linear gradient mobile phase beginning with 95:5 (v/v) water/acetonitrile and ending with 55:45 (v/v) water/acetonitrile over 22 min at a flow rate of 2.0 mL min^{-1}. The water/acetonitrile mixture contained 0.10 wt% trifluoroacetic acid (TFA). Elution traces were measured at 210 nm (dendrimer) and 491 nm (dye). The instrument was also controlled by Empower 2 software.

Absorption and emission measurements

Fluorescence and UV/Vis measurements were taken at a concentration of 0.1 mg mL^{-1} using a Fluoromax-4 (slit width 2 nm) and a Shimadzu UV-1601 UV/Vis spectrometer, respectively. For fluorescein conjugates an excitation of 491 nm and emission of 521 nm was employed. For TAMRA conjugates an excitation of 560 nm and emission of 580 nm was employed.

MALDI-TOF-MS measurements

Three solutions were prepared: 1) 10 mg mL^{-1} dendrimer in water, 2) 20 mg mL^{-1} sinnipinic acid in 1:1 acetonitrile/water, and 3) 20 mg mL^{-1} sodium trifluoroacetate in water. These were then combined in a ratio of 10:2:1 of matrix/dendrimer/salt solution. The plate was spotted with 1 μL volumes of solution and allowed to dry. At least 100 scans were averaged per measurement and a smoothing factor of 12 channels was employed.

Fluorescence quantum yield and lifetime data

Photoluminescence quantum yields (Φ_{PL}):[28] The Φ_{PL} values were recorded on a Fluoromax-4 (slit width 2.5 nm) and determined by a comparison method between a standard and sample of equal concentration and an excitation wavelength. Fluorescein samples were compared for Φ_{PL} with a standard solution of fluorescein in water at pH 11 (excitation 490 nm, $\Phi_{PL} = 0.70$). TAMRA samples were compared for Φ_{PL} with a standard solution of rhodamine-B in ethanol (excitation 560 nm, $\Phi_{PL} = 0.70$). The solutions were diluted to three sets of concentrations each with absorption ranging from 0.02–0.08, to reduce fluorimeter saturation and excimer formation. The total area of emission for each sample and standard was calculated by subtracting out the background signal and calculating the area in Origin. To obtain the best accuracy, the slope of a plot of emission versus absorption was determined and calculated according to Equation (1):

$$\Phi_{PL}(x) = \left(\frac{A_s}{A_x}\right)\left(\frac{F_x}{F_s}\right)\left(\frac{n_x}{n_s}\right)^2 \Phi_{PL}(s) \tag{1}$$

where Φ_{PL} is the quantum yield, A is the absorption at the excitation wavelength, F is the total integrated emission, and n is the refractive index of the solution, which due to low concentration, can be approximated as the refractive index of the solvent. Subscripts x and s refer to the sample and reference, respectively.

[1] D. G. Mullen, M. M. Banaszak Holl, *Acc. Chem. Res.* **2011**, *44*, 1135–1145.
[2] D. G. Mullen, M. Fang, A. Desai, J. R. Baker, B. G. Orr, M. M. Banaszak Holl, *ACS Nano* **2010**, *4*, 657–670.
[3] D. G. Mullen, A. M. Desai, J. N. Waddell, X. M. Cheng, C. V. Kelly, D. Q. McNerny, I. J. Majoros, J. R. Baker, L. M. Sander, B. G. Orr, M. M. Banaszak Holl, *Bioconjugate Chem.* **2008**, *19*, 1748–1752.
[4] L. Röglin, E. H. M. Lempens, E. W. Meijer, *Angew. Chem.* **2011**, *123*, 106–117; *Angew. Chem. Int. Ed.* **2011**, *50*, 102–112.
[5] D. G. Mullen, E. L. Borgmeier, M. Fang, D. Q. McNerny, A. Desai, J. R. Baker, B. G. Orr, M. M. Banaszak Holl, *Macromolecules* **2010**, *43*, 6577–6587.
[6] I. F. Hakem, A. M. Leech, J. D. Johnson, S. J. Donahue, J. P. Walker, M. R. Bockstaller, *J. Am. Chem. Soc.* **2010**, *132*, 16593–16598.
[7] J. F. G. A. Jansen, E. M. M. de Brabander-van der Berg, E. W. Meijer, *Science* **1994**, *266*, 1226–1229.
[8] A. W. Bosman, H. M. Janssen, E. W. Meijer, *Chem. Rev.* **1999**, *99*, 1665–1688.
[9] A. Schenning, E. Peeters, E. W. Meijer, *J. Am. Chem. Soc.* **2000**, *122*, 4489–4495.
[10] V. Balzani, P. Ceroni, S. Gestermann, M. Gorka, C. Kauffmann, F. Vogtle, *Tetrahedron* **2002**, *58*, 629–637.
[11] S. Jockusch, N. J. Turro, D. A. Tomalia, *Macromolecules* **1995**, *28*, 7416–7418.
[12] F. Puntoriero, P. Ceroni, V. Balzani, G. Bergamini, F. Vogtle, *J. Am. Chem. Soc.* **2007**, *129*, 10714–10719.
[13] G. Teobaldi, F. Zerbetto, *J. Am. Chem. Soc.* **2003**, *125*, 7388–7393.
[14] C. Ornelas, R. Lodescar, A. Durandin, J. W. Canary, R. Pennell, L. F. Liebes, M. Weck, *Chem. Eur. J.* **2011**, *17*, 3619–3629.
[15] C. Ornelas, R. Pennell, L. F. Liebes, M. Weck, *Org. Lett.* **2011**, *13*, 976–979.
[16] C. Wängler, G. Moldenhauer, R. Saffrich, E. M. Knapp, B. Beijer, M. Schnolzer, B. Wangler, M. Eisenhut, U. Haberkorn, W. Mier, *Chem. Eur. J.* **2008**, *14*, 8116–8130.
[17] A. T. Zill, K. Licha, R. Haag, S. C. Zimmerman, *New J. Chem.* **2012**, *36*, 419–427.
[18] D. Q. McNerny, J. F. Kukowska-Latallo, D. G. Mullen, J. M. Wallace, A. M. Desai, R. Shukla, B. H. Huang, M. M. Banaszak Holl, J. R. Baker, *Bioconjugate Chem.* **2009**, *20*, 1853–1859.
[19] F. Wang, W. B. Tan, Y. Zhang, X. P. Fan, M. Q. Wang, *Nanotechnology* **2006**, *17*, R1–R13.
[20] J. R. Baker, *Wiley Interdiscip. Rev. Nanomed. Nanobiotechnol.* **2013**, *5*, 423–429.
[21] Y. Kim, S. H. Kim, M. Tanyeri, J. A. Katzenellenbogen, C. M. Schroeder, *Biophys. J.* **2013**, *104*, 1566–1575.
[22] J. F. Kukowska-Latallo, A. U. Bielinska, J. Johnson, R. Spindler, D. A. Tomalia, J. R. Baker, *Proc. Natl. Acad. Sci. USA* **1996**, *93*, 4897–4902.
[23] J. Haensler, F. C. Szoka, *Bioconjugate Chem.* **1993**, *4*, 372–379.
[24] Y. Tang, Y. B. Li, B. Wang, R. Y. Lin, M. van Dongen, D. M. Zurcher, X. Y. Gu, M. M. Banaszak Holl, G. Liu, R. Qi, *Mol. Pharm.* **2012**, *9*, 1812–1821.
[25] D. G. Mullen, E. L. Borgmeier, A. Desai, M. A. van Dongen, M. Barash, X. M. Cheng, J. R. Baker, M. M. Banaszak Holl, *Chem. Eur. J.* **2010**, *16*, 10675–10678.
[26] M. A. van Dongen, A. Desai, B. G. Orr, J. R. Baker, M. M. Banaszak Holl, *Polymer* **2013**, *54*, 4126–4133.
[27] A. Salic, T. J. Mitchison, *Proc. Natl. Acad. Sci. USA* **2008**, *105*, 2415–2420.
[28] A. Maciejewski, R. P. Steer, *J. Photochem.* **1986**, *35*, 59–69.
[29] O. Varnavski, T. G. Goodson, *Chem. Phys. Lett.* **2000**, *320*, 688–696.
[30] H. Lee, T. Ooya, *J. Phys. Chem. B* **2012**, *116*, 12263–12267.
[31] M. A. van Dongen, S. Vaidyanathan, M. M. Banaszak Holl, *Soft Matter* **2013**, *9*, 11188–11196.
[32] J. E. Selwyn, J. I. Steinfeld, *J. Phys. Chem.* **1972**, *76*, 762–774.
[33] C. V. Kelly, P. R. Leroueil, E. K. Nett, J. M. Wereszczynski, J. R. Baker, B. G. Orr, M. M. Banaszak Holl, I. Andricioaei, *J. Phys. Chem. B* **2008**, *112*, 9337–9345.
[34] Y. Wang, X. B. Xie, *Nano Lett.* **2005**, *5*, 2379–2384.
[35] T. G. Goodson, *Acc. Chem. Res.* **2005**, *38*, 99–107.
[36] M. J. Cho, D. H. Choi, P. A. Sullivan, A. J. P. Akelaitis, L. R. Dalton, *Prog. Polym. Sci.* **2008**, *33*, 1013–1058.